Available online at www.sciencedirect.com
ScienceDirect
Geochimica et Cosmochimica Acta 75 (2011) 4228–4243
Geochimica et Cosmochimica Acta
www.elsevier.com/locate/gca

Fossil brines preserved in the St-Lawrence Lowlands, Québec, Canada as revealed by their chemistry and noble gas isotopes

Daniele L. Pinti [a,*], Catherine Béland-Otis [a,1], Alain Tremblay [a], Maria Clara Castro [b], Chris M. Hall [b], Jean-Sébastien Marcil [c], Jean-Yves Lavoie [c], Raynald Lapointe [a]

[a] *Département des Sciences de la Terre et de l'Atmosphère and GEOTOP, Université du Québec à Montréal, CP.8888 Succ. Centre Ville, Montréal, QC, Canada H3C 3P8*
[b] *University of Michigan, Department of Geological Sciences, 1100 N. University, C.C. Little Building, Ann Arbor, MI 48109-1005, USA*
[c] *JUNEX Inc., 2795, Boulevard Laurier, Bureau 200, QC, Canada G1V 4M7*

Received 21 December 2010; accepted in revised form 2 May 2011; available online 12 May 2011

Abstract

Brines in Cambrian sandstones and Ordovician dolostones of the St-Lawrence Lowlands at Bécancour, Québec, Canada were sampled for analysis of all stable noble gases in order to trace their origin and migration path, in addition to quantifying their residence time. Major ion chemistry indicates that the brines are of Na–Ca–Cl type, possibly derived from halite dissolution. $^{87}Sr/^{86}Sr$ ratios and Ca excess indicate prolonged interactions with silicate rocks of the Proterozoic Grenville basement or the Cambrian Potsdam sandstone. The brines constrain a 2–3% contribution of mantle ^{3}He and large amounts of nucleogenic $^{21}Ne^{*}$ and $^{38}Ar^{*}$ and radiogenic ^{4}He and $^{40}Ar^{*}$. $^{4}He/^{40}Ar^{*}$ and $^{21}Ne^{*}/^{40}Ar^{*}$ ratios, corrected for mass fractionation during incomplete brine degassing, are identical to their production ratios in rocks. The source of salinity (halite dissolution), plus the occurrence of large amounts of $^{40}Ar^{*}$ in brines constrain the residence time of Bécancour brines as being older than the Cretaceous. Evaporites in the St-Lawrence Lowlands likely existed only during Devonian–Silurian time. Brines might result from infiltration of Devonian water leaching halite, penetrating into or below the deeper Cambrian–Ordovician aquifers. During the Devonian, the basin reached temperatures higher than 250 °C, allowing for thermal maturation of local gas-prone source rocks (Utica shales) and possibly facilitating the release of radiogenic $^{40}Ar^{*}$ into the brines. The last thermal event that could have facilitated the liberation of $^{40}Ar^{*}$ into fluids and contributed to mantle ^{3}He is the Cretaceous Monteregian Hills magmatic episode. For residence times younger than the Cretaceous, it is difficult to find an appropriate source of salinity and of nucleogenic/radiogenic gases to the Bécancour brines.

1. INTRODUCTION

Calcium/chloride brines (total dissolved salinity $\geqslant$300 g/L) are ubiquitous in North American Precambrian shield and sedimentary basins (Frape et al., 2003; Kharaka et al., 2003). Although studied for more than 30 years, the origin of these extreme salinities remains enigmatic. Previous studies suggested that major solutes are leached from the crystalline host rocks over extended geologic time scales, as suggested by elevated $^{87}Sr/^{86}Sr$ ratios of 0.712–0.725 (e.g., Frape et al., 2003). However, metamorphic and magmatic rocks are not a good source of halogens. Most scholars advocated that (1) Devonian seawater evaporation and formation of a residual brine infiltrating into underlying Precambrian basement rocks (Bottomley et al.,

* Corresponding author. Tel.: +1 514 987 3000x2572; fax: +1 514 987 3635.
E-mail address: pinti.daniele@uqam.ca (D.L. Pinti).
[1] Present address: Ontario Geological Survey, Ministry of Northern Development, Mines and Forestry, Willet Green Miller Centre, Sudbury, ON, Canada P3E 6B5.

0016-7037/$ - see front matter © 2011 Elsevier Ltd. All rights reserved.
doi:10.1016/j.gca.2011.05.006

2005); or (2) the dissolution of evaporites are the dominant sources of high salinity formation waters (e.g., Carpenter, 1978; Hanor, 1994).

Here, we report noble gas results from brines with salinities varying from 94 to 315 g/L found in Cambrian–Ordovician sandstones and dolostones of the St-Lawrence Lowlands, Québec (Fig. 1). Junex Inc., a junior oil and gas exploration company operating in the Québec Appalachians foreland basin exploits these brines for commercial use. These extreme salinities are unique in sedimentary

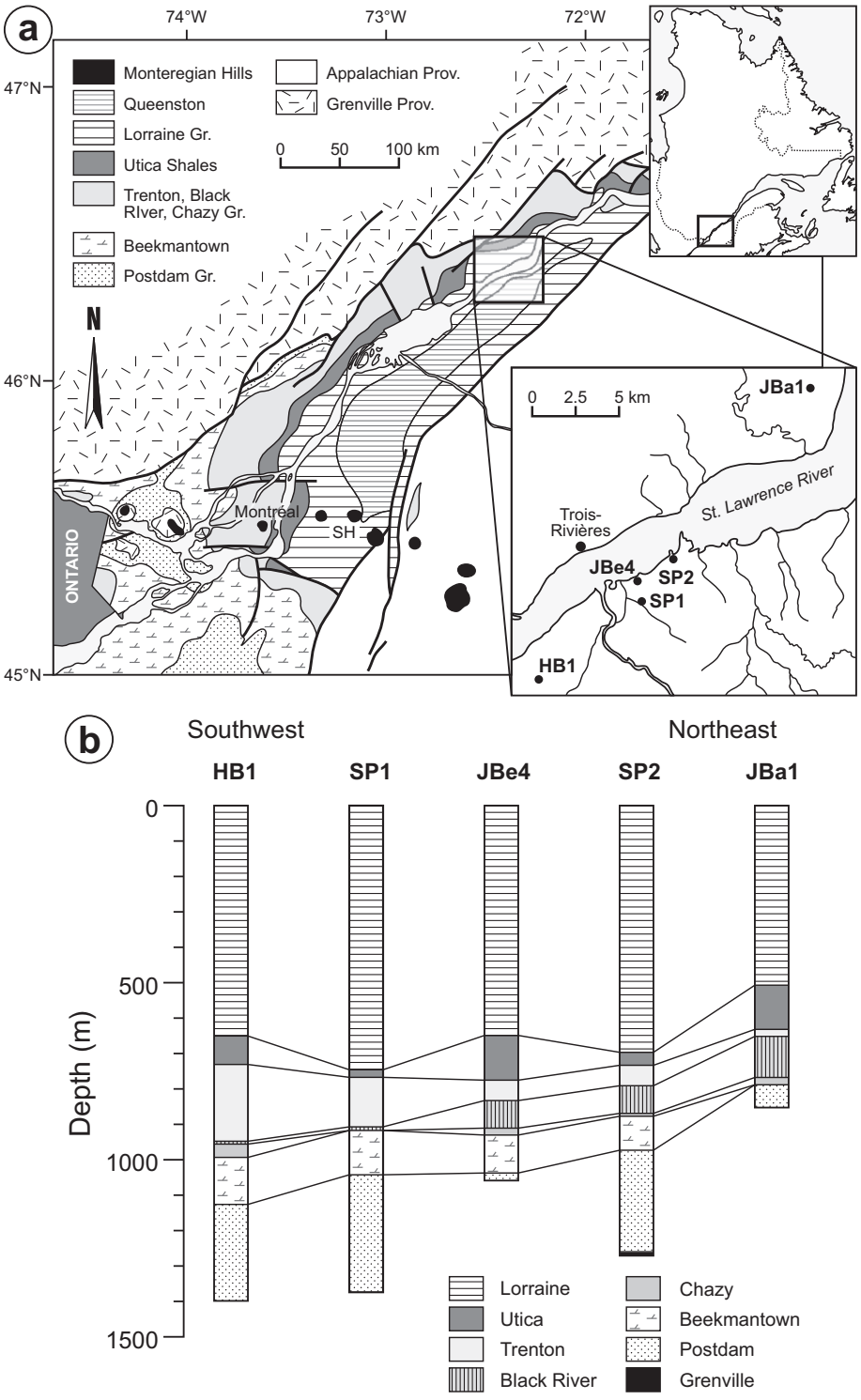

Fig. 1. (a) Geological map of St-Lawrence Lowlands and location of sampled wells at the Bécancour field. (b) Stratigraphy of Bécancour sampled wells.

formations of Québec, but they have been found in southern Ontario and northern Michigan basin (Hobbs et al., 2011). The origin, sources of solute and mechanisms of salt enrichment of the Bécancour brines is unknown and little information on their chemistry is available. Constraining the sources and residence times of these brines is of particular interest in order to: (a) assess the feasibility of creating a CO_2 repository in the area (a scenario currently explored by Junex Inc.) and; (b) shed additional light with respect to the interaction of these brines with oil/gas accumulations that might elucidate the migration of hydrocarbons the Bécancour area, a primary target for shale gas exploration in the Ordovician Utica shales.

In order to assess the origin, migration and residence time of the brines, we carried out a noble gas study in which all the stable noble gases (He, Ne, Ar, Kr, and Xe) were analyzed. Crustal fluids contain variable amounts of noble gases derived from three distinct isotopic sources: the crust, the atmosphere and the mantle. These three components can give useful information on the origin and migration of host fluids. Radiogenic isotopes ^{4}He and ^{40}Ar* are produced by decay of U, Th, and K in crustal rocks. They are released in groundwater in variable amounts, depending on their residence time (Tolstikhin et al., 1996) and basin thermal regime (Ballentine et al., 1994). Atmospheric noble gases (ANG) are dissolved in groundwater at the water table and are subsequently transported deeper in aquifers (e.g., Castro et al., 1998a,b). They can be significantly fractionated by solubility partitioning with gas or oil accumulations (Bosch and Mazor, 1988), giving an indication of mixing between fluids of differing natures. ANG are also trapped in sediments and possibly released into reservoirs during thermal (Torgersen and Kennedy, 1999) or diagenetic events (Pitre and Pinti, 2010), constituting an additional source of information on water-rock interactions. Finally, mantle noble gases, in particular primordial ^{3}He, are generally considered as a surface expression of magmatism, tectonic extension and vertical upflow of deep-seated fluids (e.g., Torgersen, 1993).

2. GEOLOGICAL BACKGROUND

The St-Lawrence Lowlands forms a relatively flat region, located between Ottawa and Québec City (Fig. 1a), filled by ca. 3000 m-thick Cambrian–Ordovician sedimentary sequence unconformably overlying the crystalline basement (granite–gneiss–anorthosite) of the Proterozoic Grenville Province. The St-Lawrence Lowlands is bounded by normal faults creating a half-graben commonly referred to as the St-Lawrence Rift System (Tremblay et al., 2003). Major tectonic events recorded in this region are (1) the opening of the Iapetus Ocean and the formation of the St-Lawrence Rift System around 550 Ma ago (Cawood et al., 2001); (2) the formation of the Appalachians between 470 and 360 Ma (Tremblay and Castonguay, 2002); (3) Middle-Late Jurassic (200–150 Ma) reactivation of the Iapetus faults during the opening of the North Atlantic Ocean (Faure et al., 1996); and (4) a Cretaceous (124 ± 10 Ma; Eby, 1985) magmatic event that produced a series of alkaline intrusions oriented approximately WNW-ESE and referred to as the Monteregian Hills (Fig. 1a). The Monteregian Hills have been interpreted as resulting from the passage of the North-American plate over the New England hotspot (Sleep, 1990) or as intrusions of magma through NW-SE Iapetus-related faults reactivated during the North-Atlantic opening (McHone, 1996).

The sedimentary rocks of the St-Lawrence Lowlands form a passive margin foreland sequence consisting of fluvial to shallow marine quartzitic sandstone deposits (Potsdam Group), marine platform dolomite and carbonates (Beekmantown, Chazy and Black River Group), detrital carbonates (Trenton), organic-rich carbonates and silty shales (Utica and Lorraine Group) and molassic shales (Queenston Group). The total thickness of the sequence is $\leqslant$3000 m, though lateral facies variations and synsedimentary faults may locally reduce drastically the thickness of the sedimentary sequence to a few hundred meters (Fig. 1b).

The Bécancour–Champlain exploration permit held by JUNEX Inc. consists of 800 km^2 on the southern (Bécancour) and northern (Champlain) embankment of the St-Lawrence River, downstream of the city of Trois-Rivières (Fig. 1a). The initial target of the field was to find accumulations of natural gas in the sedimentary layers of the Trenton/Black-River carbonate sequence. However, the reservoirs are saturated with Na–Ca–Cl brines showing salinities from 94 to 315 g/L. Sampled wells were drilled in the Potsdam sandstone, the Chazy, Beekmantown dolomites and Trenton/Black River carbonates, at depths varying from 900 to 1400 m (Table 1). Only one well, Soquip-Petrofina 2 (SP2), reaches the Grenville basement (Fig. 1b). The productive areas are all located on structural highs delimited by N–S and NE–SW faults related to the St-Lawrence Rift System.

3. SAMPLING AND ANALYTICAL METHODS

Bécancour wells are equipped with a gas/water separator at the wellhead, which allows collection of the gas phase. Noble gas samples were taken in standard refrigeration grade 3/8″ Cu tubes (~14 mL) sealed by stainless steel pinch-off clamps (Weiss, 1968) at well-head pressures after gas was allowed to flow through for several minutes. To reduce the risk of air contamination, we directly connected one extremity of the copper tube to the wellhead by using NPT connectors. Eight wells were sampled at different time periods in 2007–2008. Unfortunately, three non-productive wells (Champlain-1, Bécancour-2 and Bécancour-7) gave atmospheric noble gas compositions, though precautions were taken for sampling.

Noble gases were measured at the Noble Gas Laboratory at the University of Michigan. Gas samples were attached to a vacuum extraction system and noble gases were quantitatively extracted for inletting into a MAP-215 mass spectrometer. Extracted gases were passed over two Ti sponge getters to remove reactive gases, and sequentially allowed to enter the MAP-215 mass spectrometer using a cryo-separator. The cryo-separator temperatures were set at 30, 60, 180, 215, and 270 K for analysis of He, Ne, Ar, Kr, and Xe, respectively. The ^{4}He, ^{20}Ne, and ^{40}Ar were

Table 1
Well data and elemental and isotopic composition of brines in the region of Bécancour.

Locality/Well	Depth bottomhole (m, a.s.l.)	Density (g/cm^3)	TDS[a] (mg/L)	Na (mg/L)	K (mg/L)	Ca (mg/L)	Mg (mg/L)	Li (mg/L)	Sr (mg/L)	Cl (mg/L)	Br (mg/L)	HCO_3 (mg/L)	SO_4 (mg/L)	F (mg/L)	$^{87}Sr/^{86}Sr$ ±0.00002
Husky-Bruyère Sainte-Angèle #1	1390	1.22	314782	53250	2008	61583	1608	37	3700	192500	7.3	68	20	0.10	0.71214
Junex Batiscan #1	888	1.08	94295	12325	338	13770	847	13.9		67000			2		
Junex Bécancour #2	1265	1.13	193573	27500	630	31500	6050	13	2700	125000	4.3	160	15	0.50	0.71062
Junex Bécancour #3	936	1.13	179534	29250	560	36000	3700	10	2400	107500	4.1	89	20	0.40	0.71094
Junex Bécancour #6	999	1.14	223465	28500	715	31500	7750			155000					
Junex Bécancour #7	1064	1.13	176000	29000	500	24000	7600			114900					
Soquip-Petrofina Bécancour #1	1370	1.12	144200	7500	5100	34000	2600			95000					
Soquip-Petrofina Bécancour #2[b]	1264	1.18	240932	31915	855	52486	1417	10	2500	151590	3.5	148	8	0.21	0.71119

Internal data from JUNEX Inc.
[a] Total dissolved salinity (TDS) is recalculated as sum of the major cations and anions.
[b] Value of Br from Junex internal report of July 2004.

measured using a Faraday detector while all other isotopes were measured using an electron multiplier in ion counting mode. During neon isotope analysis, a liquid N_2 cold trap was applied to minimize peak interferences and appropriate mass peaks were monitored to correct for interferences of $^{40}Ar^{++}$ and $H_2{}^{18}O^+$ on ^{20}Ne and CO_2^{++} on ^{22}Ne. The interference corrections for ^{20}Ne and ^{22}Ne were typically ~1.1% and 0.17%, respectively. Before each sample analysis, a calibrated amount of air standard and a procedural blank were performed following the same procedure of the sample measurement. The blank correction was applied to all measured peaks, but was negligible. Isotopic abundances for each sample were normalized to the air standard after blank correction. Elemental abundances of ^4He, ^{22}Ne, ^{36}Ar, ^{84}Kr, and ^{132}Xe have typical uncertainties of 1.5%, 1.3%, 1.3%, 1.5%, and 2.2%, respectively and all uncertainties are at $\pm 1\sigma$ level. Because the extraction system at University of Michigan did not allow for pressure measurement at the point of sample inlet, the gas amount measured cannot be normalized to the total gas content. For this reason, concentrations in Table 1 have been reported as cm^3 STP and reflect the noble gas volume released from the Cu tube. Additional details on the noble gas analytical procedures can be found elsewhere (Ma et al., 2005).

4. RESULTS

4.1. Major ions and Sr isotopes of sampled brines

Major ions and strontium isotopes ($^{87}Sr/^{86}Sr$) analyzed in some of the Bécancour brines are reported in Table 1. The brines are of Na–Ca–Cl type, similar to those found in the Canadian Precambrian Shield (Frape et al., 2003) and in southern Ontario/northern Michigan basin (Hobbs et al., 2011). Conservative elements chlorine and bromine can provide constraints on the salinity source of the studied brines (e.g., Carpenter, 1978; Hanor, 1994). Fig. 2a shows measured Br^- vs. Cl^- concentrations in the Bécancour brines (black dots) in addition to those measured in brines circulating (1) in the same Cambrian–Ordovician sedimentary sequences in southern Ontario and northern Michigan basin (gray diamonds; Hobbs et al., 2011); and (2) brines from the Canadian Precambrian Shield (white circles; Frape et al., 2003). The evolution of an evaporating seawater solution is also shown, calculated after Fontes and Matray (1993). Precambrian shield and southern Ontario/northern Michigan brines are clearly derived from freshwater dilution of residual brines derived from evaporated seawater (Fig. 2a). The Bécancour brines are strongly depleted in bromine and shifted to the left side of the diagram, within the field of halite dissolution. This suggests that salinity for Bécancour derives from dissolution of evaporites, which are today absent in the St-Lawrence Lowlands sedimentary sequence.

The high calcium content of Bécancour brines (Table 1) could derive from the conversion of calcite into dolomite by magnesium-rich water (dolomitization process; Carpenter, 1978):

$$^{12}CaCO_3 + Mg^{3+} = CaMg(CO_3)_2 + Ca^{2+} \quad (1)$$

or by water–rock interactions, in particular during albitization of plagioclase, following the reaction (Davisson and Criss, 1996):

$$CaAl_2Si_2O_{8(an)} + 4SiO_2 + 2Na^+ = 2NaAlSi_3O_{8(ab)} + Ca^{2+} \quad (2)$$

To explain the Na–Ca–Cl relation in brines, Davisson and Criss (1996) presented a new type of plot, referred to as the excess-deficit plot, defined by the parameters:

$$Na_{deficit} = \frac{1}{22.99}\left(\left[\frac{Na}{Cl}\right]_{sw} \cdot [Cl]_{meas} - [Na]_{meas}\right). \quad (3)$$

$$Ca_{excess} = \frac{1}{40.08}\left([Ca]_{meas} \cdot \left[\frac{Ca}{Cl}\right]_{sw} - [Cl]_{meas}\right) \quad (4)$$

In most basinal fluids, Ca excess stoichiometrically matches the decreased Na and adheres to a 2:1 molar relationship, called the Basinal Fluid Line or BFL (Davisson and Criss, 1996; Fig. 2b). The best explanation for this relationship is that albitization of plagioclase (Eq. (2)) controls the Na and Ca abundances. Fig. 2b illustrates the relationship between $Na_{deficit}$ and Ca_{excess} calculated for the Bécancour brines and for the brines circulating in the Cambrian–Ordovician sequences in southern Ontario-northern Michigan and in the Canadian Precambrian Shield. The BFL relation of Davisson and Criss (1996) is also reported. The Bécancour brines show Ca enrichment and Na depletion, compatible with the expected relationship related to plagioclase albitization (Fig. 2b). If dolomitization was predominantly responsible for the Ca excess in the Bécancour reservoir, then a simple inverse correlation between Ca excess and Mg content should be observed, a relationship that is not apparent in our data set (Table 1). The Ca excess suggests that Bécancour brines had prolonged water-rock interactions with plagioclase-rich rocks. Those minerals are more common in the Grenville granitic-gneiss basement of Bécancour or in the derived clastic rocks of the Potsdam Group, but not in the dolomitic carbonates of the Chazy and Beekmantown Group.

The Sr isotopic composition of brines supports the existence of prolonged water-rock interaction with silicate rocks and minerals (Table 1). The $^{87}Sr/^{86}Sr$ ratios (0.71062–0.71214) measured in HB1, SPB2, JBe2 and JBe3 wells (Fig. 3) are higher than the expected Phanerozoic seawater ratio (Veizer et al., 1999) and ratios measured in Cambrian-Ordovician brines of southern Ontario/northern Michigan (from 0.7083 to 0.7106; Hobbs et al., 2011). However, they are within the values observed in brines from the Canadian Precambrian Shield (most lying between 0.712 and 0.725; McNutt et al., 1987; Frape et al., 2003). Prolonged water–rock interactions with Rb-rich and Sr-depleted silicates in relatively closed pockets, isolated from each other, as suggested by McNutt et al. (1987) and Négrel and Casanova (2005) for the Precambrian Shield brines, is a more plausible explanation of the radiogenic $^{87}Sr/^{86}Sr$ ratios measured in the Bécancour brines. The Sr isotopic composition of whole rocks and minerals measured by McNutt et al. (1987) and Franklyn et al. (1991) suggests interactions with plagioclase or K-feldspars, the latter contained in the Cambrian arkose of the Potsdam Group ($^{87}Sr/^{86}Sr$ up to 0.7330; McNutt et al., 1987).

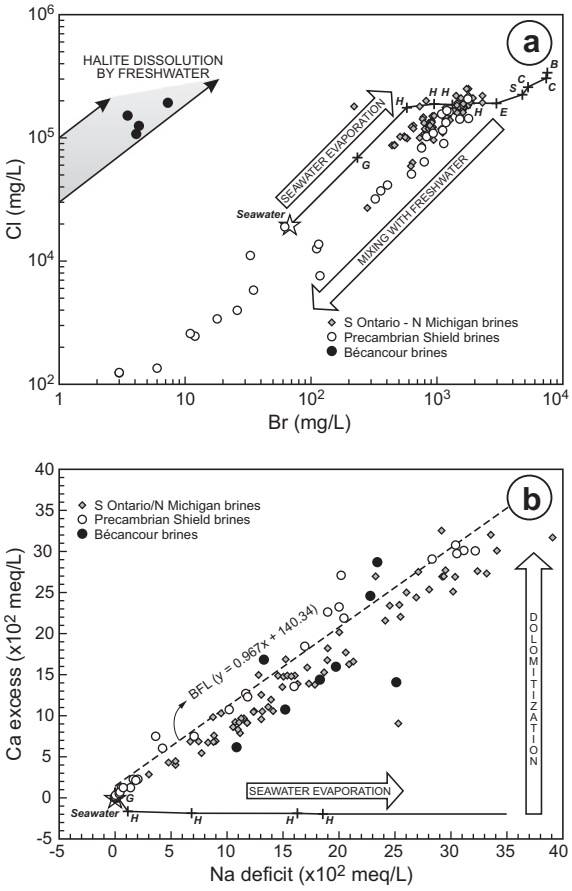

Fig. 2. (a) Br^- vs. Cl^- measured in Bécancour brines, brines of southern Ontario/northern Michigan (Hobbs et al., 2011) and of Canadian Precambrian Shield (Frape et al., 2003). The evolution of the water chemistry during the evaporation of a seawater solution (crossed line with names of precipitating salts: G = Gypsum; H = Halite; E = Epsomite; S = Sylvite; C = Carnallite; B = Bischoffite) is from Fontes and Matray (1993). (b) The Na-deficit vs. Ca-excess calculated from equations of Davisson and Criss (1996) for Bécancour, southern Ontario and Precambrian Shields brines plotted against the BFL relation in basinal fluids. Arrows indicate evolution of Ca and Na for evaporated seawater and for dolomitization processes. Symbols are as those in Fig. 2a.

4.2. Noble gases

Concentrations of ^4He, ^{20}Ne, ^{36}Ar, ^{84}Kr, and ^{132}Xe and noble gas isotopic ratios measured in the Bécancour brines are reported in Tables 2–4. Measured He isotopic ratios ($^3He/^4He = R$) were normalized to that of the atmosphere ($R_a = 1.386 \times 10^{-6}$) and corrected for air contamination following equations developed by Marty et al. (1993) and based on the $^4He/^{36}Ar$ ratios of air. Resulting $(R/R_a)_c$ values range from 0.071 to 0.174, indicating an excess of ^3He compared to pure radiogenic ratios of 0.02–0.03 Ra. The brines contain large amounts of radiogenic ^4He, as

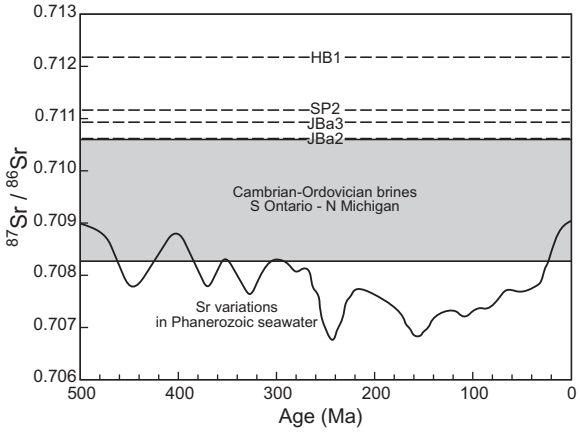

Fig. 3. The $^{87}Sr/^{86}Sr$ isotopic composition of wells JBA2, JBA3, SP2 and HB1 plotted against the curve of the isotopic Sr variations in the Phanerozoic seawater, following Veizer et al. (1999). The range of Sr isotopic compositions of brines from southern Ontario/northern Michigan (Hobbs et al., 2011) is reported for comparison.

indicated by calculated F(^{4}He) of 5000–100,000, where F(^{4}He) values are given by:

$$F(^4\mathrm{He}) = (^4\mathrm{He}/^{36}\mathrm{Ar})_{\mathrm{brines}}/(^4\mathrm{He}/^{36}\mathrm{Ar})_{\mathrm{Air}} \quad (5)$$

Fig. 4 shows the $^{20}Ne/^{22}Ne$ vs. $^{21}Ne/^{22}Ne$ ratios in Bécancour brines. Two lines have been also plotted: the MORB mixing line, which relates the atmospheric end-member ($^{20}Ne/^{22}Ne = 9.80$ and $^{21}Ne/^{22}Ne = 0.0290$) with that of the upper mantle ($^{20}Ne/^{22}Ne = 13.2$ and $^{21}Ne/^{22}Ne = 0.075$) (Sarda et al., 1988); and the crustal mixing line, which relates the atmospheric composition with that of nucleogenic production in the crust, defined on the basis of the Ne isotopic composition of natural gases from the Canadian Precambrian Shield, Alberta, New Mexico and SW USA (gray open circles in Fig. 4; Kennedy et al., 1990). Bécancour brines (black closed circles, Fig. 4) display two different patterns. With the exception of Soquip-Petrofina Bécancour 2 (SP2), most samples display $^{20}Ne/^{22}Ne$ and $^{21}Ne/^{22}Ne$ ratios greater than the atmospheric value with Ne isotopic compositions close to the MORB-Air mixing line (Fig. 4). The Ne isotopic composition of SP2 clearly shows excesses of both ^{21}Ne and ^{22}Ne, pointing to a contribution of crustal Ne, mainly from the nucleogenic reactions $^{18}O(\alpha,n)^{21}Ne$ and $^{19}F(\alpha,n)^{22}Ne$ (Wetherill, 1954).

$^{40}Ar/^{36}Ar$ ratios of the Bécancour brines are also greater than the atmospheric value (295.5) and range from 369.7 to 2110.5 (Table 2), indicating the accumulation of large amounts of radiogenic $^{40}Ar^*$. $^{38}Ar/^{36}Ar$ ratios range from 0.1876 ± 0.0010, identical to the atmospheric value of 0.1880 up to 0.2162 ± 0.0118. The apparent excess of ^{38}Ar compared to the atmospheric value is related to excesses of ^{21}Ne as discussed in detail below.

Krypton and xenon isotopic compositions are atmospheric within uncertainties (Table 3) and the few isotopic variations observed can be accounted mainly by for mass fractionation. This is well evidenced by the co-variation between $^{129}Xe/^{132}Xe$ and $^{131}Xe/^{132}Xe$ (Fig. 5a). Interestingly, a correlation between $^{20}Ne/^{22}Ne$ and $^{131}Xe/^{132}Xe$ (Fig. 4b), as well as a rough inverse relation with $^{86}Kr/^{84}Kr$ (Fig. 5c) suggests that the observed slight ^{20}Ne excesses are related to mass fractionation rather than the addition of a neon mantle component (Fig. 4).

5. DISCUSSION

5.1. Brine degassing and air addition

$^{20}Ne/^{22}Ne$ ratios higher than the atmospheric value are likely related to isotopic fractionation by gaseous diffusion as suggested by its relation with Kr and Xe isotopes (Fig. 5b and c). This fractionation could be created during well pumping and partial gas phase separation at the wellhead. This phenomenon could also be responsible for variations in noble gas concentrations observed in the same well sampled at different periods (Tables 2–4).

If partial degassing of the brine occurred, lighter isotopes will preferentially escape to the residual gaseous phase, following a Rayleigh distillation (e.g., Matsumoto et al., 2004):

$$\left(\frac{^{20}\mathrm{Ne}}{^{22}\mathrm{Ne}}\right)_{\mathrm{escaped}} = \left(\frac{^{20}\mathrm{Ne}}{^{22}\mathrm{Ne}}\right)_0 \cdot \frac{1-f^{\alpha}}{1-f} \quad (6)$$

where f is the fraction of gas retained in the brine, and $(^{20}Ne/^{22}Ne)_0$ is the initial isotopic value in the brine prior to degassing. For a diffusion-controlled process, the fractionation factor α is given by $\sqrt{22/20}$ (Marty, 1984). From Eq. (6), the initial isotopic ratio will vary between two limits: $f \to 1$ the $(^{20}Ne/^{22}Ne)_{\mathrm{escaped}} \to (^{20}Ne/^{22}Ne)_0 \times \alpha$; for $f \to 0$ the $(^{20}Ne/^{22}Ne)_{\mathrm{escaped}} \to (^{20}Ne/^{22}Ne)_0$, i.e., if the brine is completely degassed at the wellhead, no isotopic fractionation should be observed.

Fig. 6 shows the relative abundances of Ar, Kr and Xe as a function of F(i) values, which correspond to the fractionation factors relative to atmospheric composition as given by Eq. (5) (in which ^{84}Kr and ^{132}Xe replace ^{4}He). F(^{84}Kr) and F(^{132}Xe) values expected for a freshwater component (ASW at 10 °C) and for brines at well conditions (Air Saturated Brine or ASB with salinities varying between 240 and 315 g/L for $T = 50$ °C) have also been calculated and plotted (Fig. 6) using solubility data from Smith and Kennedy (1983). Three degassing curves have also been plotted with two representing F(^{84}Kr) and F(^{132}Xe) variations for a diffusion- (curve with white dots) and solubility-controlled degassing process (dashed curve with gray squares) of a brine at well-head conditions. The third one (dashed curve with black dots) represents the degassing of an air component.

For a diffusion-controlled degassing process, the lighter isotope ^{36}Ar will be preferentially released with respect to heavier ^{84}Kr and ^{132}Xe, fractionating F(i) toward lower values than those expected by the ASB conditions, following the equation (e.g., Ma et al., 2009):

$$\left(\frac{i}{^{36}\mathrm{Ar}}\right)_{\mathrm{escaped}} = \left(\frac{i}{^{36}\mathrm{Ar}}\right)_0 \cdot \frac{1-f^{\alpha}}{1-f} \quad (7)$$

Table 2
Elemental and isotopic composition of He, Ne and Ar in Bécancour brines.

Locality/well	[^{4}He] cm^3 STP	±1σ	[^{20}Ne] cm^3 STP	±1σ	[^{36}Ar] cm^3 STP	±1σ	^{3}He/^{4}He R/Ra	^{3}He/^{4}He$_c$ R/Ra$_c$ corrected	±1σ	^{20}Ne/^{22}Ne	±1σ	^{21}Ne/^{22}Ne	±1σ	^{38}Ar/^{36}Ar	±1σ	^{40}Ar/^{36}Ar	±1σ
	×10^{-2}		×10^{-6}		×10^{-6}												
Husky-Bruyère Sainte-Angèle #1																	
HB1 07-1B	1.80	0.03	3.45	0.04	4.12	0.05	0.095	0.095	0.007	10.12	0.04	0.0311	0.0002	0.1908	0.0017	1162.0	8.1
HB1 07-3B	2.74	0.04	0.89	0.01	1.78	0.02	0.111	0.111	0.008	10.07	0.06	0.0343	0.0003	0.1936	0.0019	2110.5	15.5
Junex Batiscan #1																	
JBa1 07-3B	1.98	0.03	12.61	0.16	23.56	0.31	0.085	0.085	0.005	9.85	0.08	0.0294	0.0003	0.1876	0.0010	369.7	1.6
Junex Bécancour #4																	
JBe4 07-2C	1.68	0.03	0.83	0.01	1.16	0.02	0.071	0.071	0.005	10.18	0.16	0.0340	0.0006	0.1979	0.0024	1309.0	10.6
Soquip-Pètrofina Bécancour #1																	
SP1 07-2B	1.13	0.02	2.05	0.03	3.52	0.05	0.100	0.100	0.009	10.08	0.06	0.0314	0.0003	0.1981	0.0042	988.4	17.5
SP1 07-2C	1.64	0.02	1.40	0.02	1.94	0.03	0.079	0.079	0.004	10.20	0.05	0.0320	0.0003	0.1928	0.0019	1498.0	8.9
Soquip-Pètrofina Bécancour #2																	
SP2-07-3A	71.03	1.07	1.58	0.02	42.99	2.02	0.174	0.174	0.010	8.67	0.15	0.0672	0.0011	0.2162	0.0118	1104.9	53.3
SP2-07-3B	64.35	0.97	3.34	0.06	38.97	0.51	0.072	0.072	0.030	8.38	0.18	0.0620	0.0009	0.1982	0.0025	1818.3	18.9
Air[a]								1.000		9.80		0.0290		0.1880		295.5	

[a] Data from Ozima and Podosek (1983).

Table 3
Elemental and isotopic composition of Kr in Bécancour brines.

Locality/well	$[^{84}Kr]$ cm^3 STP $\times 10^{-8}$	$\pm 1\sigma$	$^{80}Kr/^{84}Kr$	$\pm 1\sigma$	$^{82}Kr/^{84}Kr$	$\pm 1\sigma$	$^{83}Kr/^{84}Kr$	$\pm 1\sigma$	$^{86}Kr/^{84}Kr$	$\pm 1\sigma$
Husky-Bruyère Sainte-Angèle #1										
HB1 07-1B	6.30	0.09	0.04079	0.00054	0.20030	0.00215	0.19990	0.00237	0.30400	0.00383
HB1 07-3B	3.17	0.05	0.04558	0.00065	0.20045	0.00323	0.19960	0.00345	0.30786	0.00564
Junex Batiscan #1										
JBa1 07-3B	48.57	0.73	0.03997	0.00018	0.20313	0.00082	0.20230	0.00077	0.30745	0.00182
Junex Bécancour #4										
JBe4 07-2C	2.67	0.04	0.04111	0.00059	0.20200	0.00192	0.20060	0.00230	0.30310	0.00332
Soquip-Petrofina Bécancour #1										
SP1 07-2B	5.67	0.10	0.04915	0.00125	0.20150	0.00458	0.20130	0.00575	0.30360	0.00729
SP1 07-2C	4.10	0.06	0.04194	0.00055	0.20410	0.00196	0.20230	0.00186	0.30220	0.00407
Soquip-Petrofina Bécancour #2										
SP2-07-3A	68.50	2.88	0.05605	0.00267	0.19726	0.01290	0.19754	0.01222	0.30751	0.01828
SP2-07-3B	48.57	0.73	0.04200	0.00089	0.20255	0.00254	0.20270	0.00281	0.30617	0.00501
Air[a]			0.03960	–	0.20217	–	0.20136	–	0.30524	–

[a] Data from Ozima and Podosek (1983).

where f is the fraction of ^{36}Ar in the retained phase after degassing occurred. For a diffusion-controlled process, the fractionation coefficient α is given by:

$$\alpha = D_i/D_{Ar} \quad (8)$$

where D is the noble gas diffusion coefficient in water calculated as cm^2 s^{-1} (Jähne et al., 1987). Because solubility of noble gases in water differs and follows the trend He < Ne < Ar < Kr < Xe, during partial degassing, the sampled gas phase should also be enriched in ^{36}Ar (less soluble) compared to ^{84}Kr and ^{132}Xe (more soluble species). For a solubility-controlled degassing, the fractionation coefficient α is given by:

$$\alpha = K_{Ar}/K_i \quad (9)$$

where K_{Ar} and $K_{i(Kr,Xe)}$ are the solubility constants for noble gases as calculated by Smith and Kennedy (1983) and given in atm kg mol^{-1}.

A simple degassing of ASB cannot explain the fractionated $^{84}Kr/^{36}Ar$ and $^{132}Xe/^{36}Ar$ values measured in the Bécancour brines (Fig. 6). Similarly, mixing between an ASB or ASB-degassed fluid and the atmosphere cannot explain our fractioned ratio values neither. However, from Fig. 6 it appears that air addition in the well prior to degassing might lead to the observed anomalously low F(^{84}Kr) and F(^{132}Xe) values. This suggests that air addition in the Bécancour wells could be ubiquitous, as previously observed in the wells Champlain-1 and Bécancour-2 and 7 (see Section 3).

It is also conceivable that during water-rock interactions, atmospheric noble gases trapped in sedimentary rocks are released into water. Such a release is an alternative hypothesis to explain fractionation factors of the heavier noble gases less than unity. Matsuda and Nagao (1986) and Matsuda and Matsubara (1989) measured atmospheric noble gases in marine sediments and found ^{36}Ar, ^{84}Kr and ^{132}Xe average concentrations of 1.3×10^{-7}, 1.9×10^{-8}, and 2.3×10^{-9} ccSTP/g$_{rock}$. Assuming a 5% porosity rock with an average density of 2.7 g/cm^3, the amounts of atmospheric noble gases trapped in sediments that could be released into a 5.4 wt% brine are 15%, 1330%, and 1550% times their initial dissolved amount for ^{36}Ar, ^{84}Kr and ^{132}Xe, respectively. Assuming that transfer of noble gases from rock to fluids is governed by diffusion with diffusion coefficients of He > Ne > Ar > Kr > Xe, we can speculate that the release of atmospheric noble gases from sedimentary rocks into fluids might lead to the observed extremely depleted fractionation values of the heavier noble gases (Fig. 6). So far, however, the release of atmospheric noble gases into fluids in relation to diagenetic processes or water–rock interactions has been documented in only two studies. The first is the contribution of ANG from source rocks to hydrocarbons at the Elk Hills Naval Petroleum Reserve, CA (Torgersen and Kennedy, 1999). The second study documents the release of large amounts of ANG to pore water from estuarine sediments of the St-Lawrence River, Québec (Pitre and Pinti, 2010). In both cases, desorption of ANG trapped on clay surfaces rather than diffusion seems to be the main mechanism responsible for the release of ANG to fluids. Because adsorption of

Table 4
Elemental and isotopic composition of Xe in Bécancour brines.

Locality/well	$[^{132}Xe]$ cm^3 STP $\times 10^{-9}$	±1σ	$^{128}Xe/^{132}Xe$	±1σ	$^{129}Xe/^{132}Xe$	±1σ	$^{130}Xe/^{132}Xe$	±1σ	$^{131}Xe/^{132}Xe$	±1σ	$^{134}Xe/^{132}Xe$	±1σ	$^{136}Xe/^{132}Xe$	±1σ
Husky-Bruyère Sainte-Angèle #1														
HB1 07-1B	2.63	0.06	0.07341	0.00191	0.9903	0.0088	0.1498	0.0024	0.7949	0.0082	0.3916	0.0050	0.3445	0.0056
HB1 07-3B	1.79	0.04	0.06998	0.00161	0.9835	0.0104	0.1525	0.0024	0.7891	0.0107	0.3978	0.0066	0.3359	0.0058
Junex Batiscan #1														
JBa107-3B	20.06	0.44	0.07119	0.00077	0.9802	0.0074	0.1504	0.0016	0.7863	0.0058	0.3871	0.0036	0.3319	0.0032
Junex Bécancour #4														
JBe4 07-2C	1.41	0.03	0.06937	0.00160	0.9741	0.0110	0.1490	0.0028	0.7907	0.0094	0.3921	0.0057	0.3332	0.0058
Soquip-Petrofina Bécancour #1														
SP1 07-2B	3.37	0.07	0.07036	0.00208	0.9803	0.0235	0.1510	0.0042	0.7879	0.0195	0.3928	0.0097	0.3332	0.0079
SP1 07-2C	2.92	0.06	0.07092	0.00109	0.9905	0.0085	0.1501	0.0016	0.7937	0.0067	0.3956	0.0041	0.3388	0.0036
Soquip-Petrofina Bécancour #2														
SP2-07-3A	38.67	1.66	0.06719	0.00443	0.9471	0.0581	0.1445	0.0092	0.7762	0.0465	0.3835	0.0241	0.3384	0.0201
SP2-07-3B	50.90	1.12	0.07126	0.00174	0.9721	0.0133	0.1481	0.0025	0.7837	0.0108	0.3982	0.0055	0.3411	0.0065
Air[a]			0.07136	–	0.9832	–	0.1514	–	0.7890	–	0.3879	–	0.3294	–

[a] Data from Ozima and Podosek (1983).

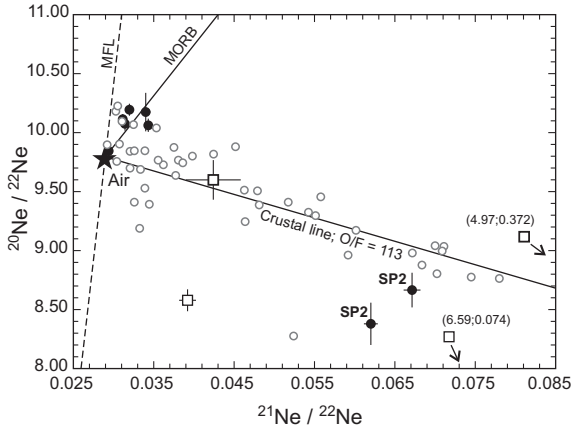

Fig. 4. The 3-isotope plot of neon ($^{20}Ne/^{22}Ne$ vs. $^{21}Ne/^{22}Ne$) of Bécancour brines. The MORB line represents mixing between atmospheric neon and that measured in the upper mantle (Sarda et al., 1988). The crust line represents the evolution of neon isotopic composition by nucleogenic production of ^{20}Ne,^{21}Ne,$^{22}Ne^*$ in a crustal source having constant O/F ratio of 113 (Kennedy et al., 1990). Gray dots represent the Ne isotopic composition of North America natural gases (Kennedy et al., 1990). White squares are the Ne isotopic ratios measured in Monteregian Hills magmatic rocks (Sasada et al., 1997). MFL is the mass fractionation line depicting the isotopic variations of Ne produced by a diffusion-controlled degassing process.

noble gases increases with atomic number increase (Fanale and Cannon, 1972), fluids show very large F(Kr) and F(Xe), ~10–100 times higher than their solubility values in seawater (Pitre and Pinti, 2010), rather than the depleted values observed in our samples (Fig. 6). Alternatively, during evaporite dissolution and brine formation (Fig. 2a), released ANGs dissolved into water. However, this "excess air" should produce F(Kr) and F(Xe) approaching unity, i.e., simple air, rather than values less than unity (Fig. 6). It is interesting to note that in the only documented noble gas study of brines in the Canadian Precambrian Shield (Greene et al., 2008), the calculated F(Kr) and F(Xe) are lower than unity and range from 0.15 to 0.62 and from 0.25 to 1.05, respectively. This might suggest that brines typically display depleted F(*i*) values. Although appealing, additional data and in-depth studies on ANG fractionation processes are required to investigate the veracity of such a hypothesis.

5.2. ^{3}He sources

The atmosphere-corrected helium isotopic ratios of Bécancour brines ($R/Ra_c = 0.071–0.174$) are higher than typical crustal values (0.02–0.03 Ra) that result from thermal neutron capture by lithium ($^6Li(n,\alpha) \rightarrow {}^3H(\beta) \rightarrow {}^3He$) and $^{238,235}U$ and ^{232}Th α-decay (^4He) (Andrews and Kay, 1982). In Fig. 7, we report $^3He/^{21}Ne^*$ plotted against $^4He/^{21}Ne^*$ ratios. There is a rough exponential relationship between $^3He/^{21}Ne^*$ and $^4He/^{21}Ne^*$, which might be accounted for by the addition of 2–3% mantle ^3He. Alternatively, nucleogenic ^3He production from Li contained in rocks (Wetherill, 1954) might have taken place.

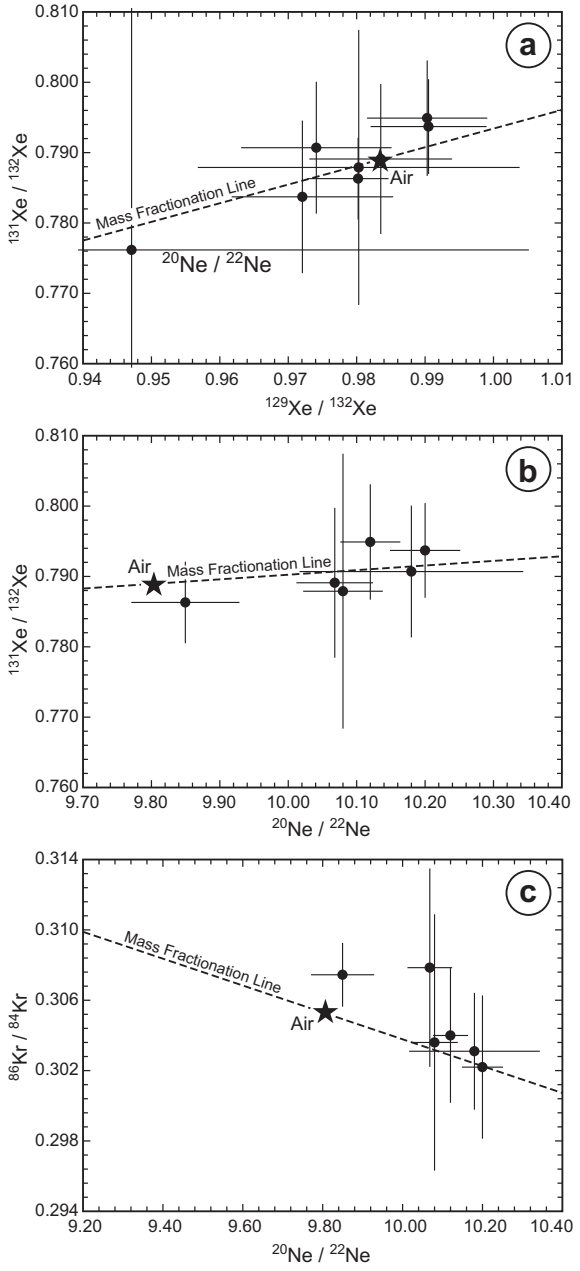

Fig. 5. (a) The ^{129}Xe/^{132}Xe vs. the ^{131}Xe/^{132}Xe ratios in Bécancour brines (black dots). The isotopic variations, close to that of the atmospheric xenon can be explained by simple mass fractionation (dashed line). (b) The ^{20}Ne/^{22}Ne vs. ^{131}Xe/^{132}Xe and (c) vs. ^{86}Kr/^{84}Kr ratios. Isotopic variations can be explained by mass fractionation of a degassed phase (dashed line).

Li content in Bécancour brines range from 6.9 to 37 ppm (Table 1). Li content in sedimentary rocks of the St-Lawrence Lowlands and the crystalline rocks of Grenville are in the same range as those of the Bécancour brines (Table 5). Assuming a maximum Li value of 37 ppm in brines, average U and Th contents in Postdam sandstone, Beekmantown and Chazy dolomites or Grenville gneiss-amphibolitic crystalline rocks (Table 5) and relevant equations by Andrews and Kay (1982), leads to terrigenic

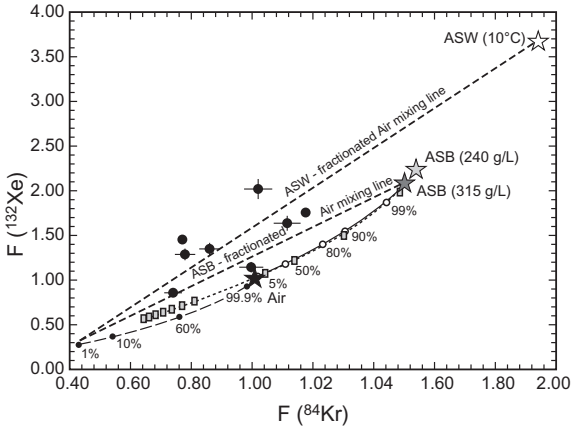

Fig. 6. Fractionation factors F(^{84}Kr) vs. F(^{132}Xe) as calculated in the Bécancour brines. End-member compositions of atmospheric noble gases in brines (ASB or Air Saturated Brine) have been calculated for reservoir temperature of 50 °C and salinity ranging from 240 g/L (SP2 well) and 315 g/L (HB1 well). Air saturated water (ASW at 10 °C) is assumed for recharge freshwater. Two curves represent the evolution of fractionation factors for Kr and Xe during a diffusion–(continuous curve with white circles) and a solubility-controlled (dashed curve with gray squares) degassing of brine at initial ASB condition. One more curve (dashed with black circles) has been calculated for a degassing of a brine containing an atmospheric contaminated component (F(^{84}Kr) = F(^{132}Xe) = 1). Numbers represent the percentages of degassing. Straight dashed lines represent mixing between a recharge freshwater component and ASB brine and a fractionated atmospheric component.

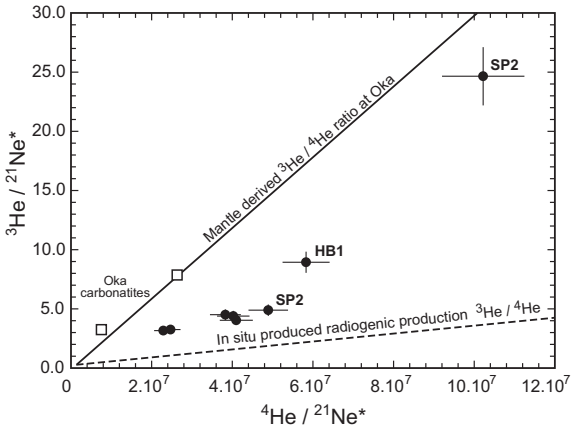

Fig. 7. The ^{3}He/^{21}Ne* vs. ^{4}He/^{21}Ne* ratios in Bécancour brines (black dots). The slope of the dashed line represents the ^{3}He/^{4}He ratio produced *in situ* by nucleogenic (^{3}He, ^{21}Ne*) and radiogenic (^{4}He) reactions in average crustal reservoir rocks. The slope of the plain line represents the average ^{3}He/^{4}He ratio measured in Monteregian Hills magmatic rocks (white squares; Sasada et al., 1997).

^{3}He/^{4}He ratios between 0.003 and 0.026 Ra (Fig. 7, dashed line). This is far below our measured maximum value of 0.174 Ra (Table 2; Fig. 7). Li content up to 4000 ppm would be required to produce the high measured ^{3}He/^{4}He ratios. Such high Li values are uncommon in crustal rocks of average composition (Mamyrin and Tolstikhin, 1984).

Table 5
Chemistry of Lowlands sedimentary rocks, Grenville crystalline rocks and Monteregian Hills magmatic rocks, together with radiogenic/nucleogenic production rates and ratios.

Lithology	O (wt%)	Mg (wt%)	Cl (ppm)	F (ppm)	U (ppm)	Th (ppm)	K (ppm)	Li (ppm)	Neutrons (g^{-1} vr^{-1})	^{3}He ($\times10^{-21}$)	^{4}He ($\times10^{-14}$)	$^{21}Ne^{*}$ ($\times10^{-21}$)	$^{22}Ne^{*}$ ($\times10^{-21}$)	$^{36}Ar^{*}$[a] ($\times10^{-21}$)	$^{38}Ar^{*}$ ($\times10^{-23}$)	$^{40}Ar^{*}$ ($\times10^{-14}$)	$^{3}He/^{4}He$ R/Ra	$^{4}He/^{40}Ar^{*}$	$^{21}Ne^{*}/^{40}Ar^{*}$ ($\times10^{-7}$)	$^{4}He/^{21}Ne^{*}$ ($\times10^{-7}$)	$^{3}He/^{21}Ne^{*}$
Monteregian Hills																					
Gabbro	41.9	4.3	263	587	0.3	3.1	4900	28	2.3	1.7	12.2	4.1	1.2	0.4	1.4	1.9	0.019	6.5	2.2	2.9	0.412
Pyroxenite	40.3	5.5	–	–	1.9	2.6	5065	11	4.1	1.7	30.8	13.6	–	1.6	–	1.9	0.008	16.0	7.1	2.3	0.124
Diorite	43.2	1.8	231	483	2.5	12.1	18870	37	13.0	12.0	65.0	25.9	6.1	2.2	7.3	7.2	0.026	9.1	3.6	2.5	0.465
Grenville																					
Gneiss	48.7	0.6	354	394	2.2	9.0	17641	19	8.3	5.0	52.4	24.0	4.1	4.5	9.2	6.7	0.013	7.8	3.6	2.2	0.207
Quartzite	52.0	0.1	88	215	2.5	10.0	7059	12	8.5	3.5	58.9	28.9	2.5	4.6	2.6	2.7	0.008	21.9	10.8	2.0	0.122
Amphibolite	44.6	3.4	–	–	0.3	1.3	4634	9	1.2	0.3	7.2	3.0	–	–	–	1.8	0.006	4.1	1.7	2.4	0.107
Lowlands																					
Dolomite	45.0	10.8	480	224	2.0	7.5	4572	5	4.3	1.1	45.7	20.0	2.2	2.6	11.0	1.7	0.003	26.3	11.5	2.3	0.057
Limestone	45.4	1.1	255	321	1.6	4.7	6250	7	3.1	1.2	32.7	14.7	2.2	1.9	4.3	2.4	0.005	13.8	6.2	2.2	0.080
Sandstone	53.1	0.01	–	–	0.4	1.4	3089	19	0.8	0.8	9.0	4.6	–	0.3	–	1.2	0.013	7.7	3.9	1.9	0.183
Upper crust	47.5	1.13	232	–	2.8	10.7	28200	20	11.2	6.4	64.5	29.2	58.4	7.1	7.5	10.7	0.014	6.0	2.7	2.2	0.221
Brine		0.39	126061	0.3	0.12	0.0	1338	17	0.1	0.1	1.4	0.0005	0.0003	3.1	115.0	0.5	0.012	2.8	0.001	2912	247
													ccSTP g^{-1}_{H2O}								
										$\times10^{-14}$			$\times10^{-9}$			$\times10^{-6}$					
Brine[b]										1.8	12.9	0.1	4.3	141.6	27	41.8					

Data sources. Monteregian Hills: (Eby, 1985) excepted Li content calculated as average on 115 rock analyses from SIGEOM database from the Québec Ministry of Environment. Grenville: Chemical composition calculated as average on 196 rock analyses from the SIGEOM database. St-Lawrence Lowlands: Dolomite and carbonate composition calculated as average from 398 rock analyses from the SIGEOM database. Potsdam quartzitic sandstone composition (labeleld simply "sandstone") is from Owen and Greenough (2008) and Rivard et al. (2002) except for Li content calculated as average on 10 quartzitic sandstone analyses from the SIGEOM database.

Upper crust: Table 8 in Ballentine and Burnard (2002). Brine: average of dissolved ions measured in the Bécancour brines (from Table 1 data). U content has been measured at GEOTOP by B. Ghaleb in Husky Bruyeres #1 well. Th is assumed to be practically zero because it is not soluble in brines. U and Th data are in the range of reported by Andrews et al. (1989) for an evaporite ($U = 0.1$ ppm and $Th = 1 \times 10^{-5}$ ppm).

[a] $^{36}Ar^{*}$ production rates have been calculated using equation from Fontes et al. (1991). Neutron production rates for sandstone, limestone, gabbro and gneiss are average values from Andrews et al. (1989). Thermal neutron capture probability of ^{35}Cl in brine has been calculated using equations of Andrews and Kay (1982) and for rock matrices from Table 1 of Ballentine and Burnard (2002).

[b] Concentrations of isotopes in an initial Bécancour brine, before the *in situ* production of nucleogenic/radiogenic isotopes. Concentrations calculated for a brine with a maximum salinity of 5.4 M of NaCl and a reservoir temperature of 50 °C, using solubility data from Smith and Kennedy (1983).

Although some alkaline intrusions of the Monteregian Hills, such as the Mt St-Hilaire (labeled SH in Fig. 1a) contain unusually high Li-rich minerals such as the phosphate Nalipoite (22 wt% LiO_3; Chao and Ercit, 1991), it is unlikely that this localized mineralization could produce noticeable amounts of nucleogenic ^3He to large volumes of sedimentary fluids. We thus conclude that nucleogenic ^3He cannot be produced from thermal neutron capture by lithium neither in the brines, nor in the sedimentary reservoir rocks.

Mantle-derived ^3He has been found in several localities of the eastern north-American passive margin. Shallow groundwater from the Mirror Lake aquifer, New Hampshire contains appreciable amounts of mantle helium (Torgersen et al., 1995) with R/Ra of 1.65 ± 0.10 (where $R = {}^3He/{}^4He$ normalized to the atmosphere ratio $Ra = 1.386 \times 10^{-6}$). Siegel et al. (2004) measured R/Ra from 0.35 to 0.44 in brines from Saratoga Springs NY, indicating a 4–5% contribution of mantle ^3He. Castro et al. (2009) found primordial He in deep brines of the Michigan Basin, with R/Ra values up to 1.29. Torgersen et al. (1995) hypothesized that the New England hotspot could have been the source of mantle ^3He found at Mirror Lake, NH. Occurrence of $^3He/^4He$ ratios of 0.21–0.25 Ra measured in carbonatites of the Monteregian Hill Oka complex (Sasada et al., 1997; Fig. 7) suggests that a very old mantle helium signature has been preserved in the region, possibly affecting the Bécancour brines.

5.3. Origin of nucleogenic ($^{38}Ar^*$, $^{21}Ne^*$) and radiogenic (^4He, $^{40}Ar^*$) components

$^{21}Ne/^{22}Ne$ ratios measured in the Bécancour brines are positively correlated with $^{38}Ar/^{36}Ar$ ratios (Fig. 8). With the exception of Soquip Petrofina 2 samples, which are shifted towards higher $^{21}Ne/^{22}Ne$ values (right side of the diagram), this correlation is particularly good. Excesses of ^{38}Ar compared to the atmospheric $^{38}Ar/^{36}Ar$ ratio of 0.1880 can be produced by nucleogenic reactions with chlorine given by $^{35}Cl(\alpha,p)^{38}Ar$ (Wetherill, 1954). Although some natural gas shows $^{38}Ar/^{36}Ar$ ratios in excess of air ratios, anomalies of ^{38}Ar in crustal solids or fluids are rare and often related to mass fractionation (Marty, 1984). Correlated anomalies of nucleogenic $^{21}Ne^*$ and $^{38}Ar^*$ have so far been only unequivocally observed in Archean cherts (dashed line in Fig. 8; Sano et al., 1994).

Mass fractionation is not responsible for the measured ^{38}Ar anomalies (and implicitly ^{21}Ne) because if large isotopic fractionation of argon had occurred, an inverse correlation between $^{38}Ar/^{36}Ar$ and $^{21}Ne/^{22}Ne$ ratios would be observed and this is not the case for our brines (Fig. 8). In situ production of $^{21}Ne^*$ and $^{22}Ne^*$ should be low in brines because of the small neutron production rate and Mg and F contents (Table 5). The production of $^{36}Ar^*$ dominates over that of $^{38}Ar^*$ because of the large Cl contents. The resulting $^{38}Ar/^{36}Ar$ and $^{21}Ne/^{22}Ne$ ratios are indistinguishable from the atmospheric values.

In Fig. 8, we report the evolution of $^{38}Ar/^{36}Ar$ and $^{21}Ne/^{22}Ne$ ratios (plain line labeled "production in the reservoir") in the dolomitic reservoir due to the addition of

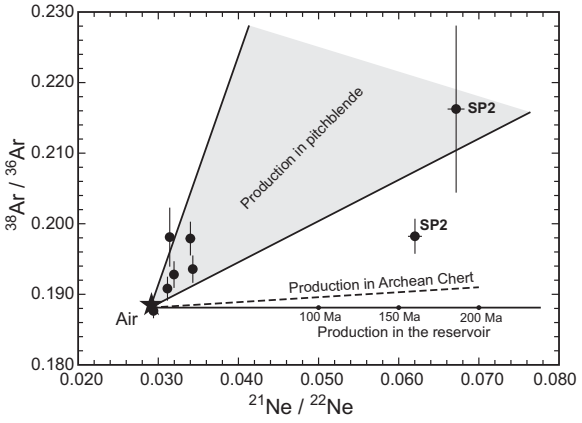

Fig. 8. The $^{21}Ne/^{22}Ne$ vs. $^{38}Ar/^{36}Ar$ measured in the Bécancour brines. The atmospheric Ne and Ar composition is also reported. The lower plain line represents the evolution of an atmospheric Ne and Ar signal by addition of nucleogenic-produced $^{35}Cl(\alpha,p)^{38}Ar$, $^{36}Cl(n,\gamma),\beta^{-36}Ar$, $^{18}O(\alpha,n)^{21}Ne$, $^{19}F(\alpha,n),\beta^{+22}Ne$, $^{19}F(\alpha,p)^{22}Ne$, $^{24}Mg^{25}Mg(n,\alpha)^{21}Ne,^{22}Ne$ in the dolomite reservoir, taken as an example. Numbers are calculated residence time of the brine (Eq. (6) in the text) needed to acquire the expected Ar and Ne isotopic ratios. The dashed line represents the production ratio of $^{38}Ar^*$ and $^{21}Ne^*$ as calculated in Archean cherts by Sano et al. (1994). The gray field indicates the expected Ar and Ne isotopic composition produced in U–Th–Cl–F rich accessory minerals, such as pitchblende (taken as an example) as measured by Eikenberg et al. (1993).

nucleogenic-produced $^{35}Cl(\alpha,p)^{38}Ar$, $^{36}Cl(n,\gamma)$, $\beta^{-36}Ar$, $^{18}O(\alpha,n)^{21}Ne$, $^{19}F(\alpha,n)$, $\beta^{+22}Ne$, $^{19}F(\alpha,p)^{22}Ne$, $^{24}Mg^{25}$-$Mg(n,\alpha)^{21}Ne,^{22}Ne$ (Eikenberg et al., 1993), following the equation:

$$\frac{x}{y} = \frac{C^x_{ASB} + P^x \times \frac{\rho r}{\rho w} \times \Lambda \times \left[\frac{1-\phi}{\phi}\right] \times t}{C^y_{ASB} + P^y \times \frac{\rho r}{\rho_w} \times \Lambda \times \left[\frac{1-\phi}{\phi}\right] \times t} \quad (10)$$

where x and y denote ^{21}Ne, ^{38}Ar and ^{22}Ne, ^{36}Ar isotopes, respectively. $C^{x,y}_{ASB}$ is the initial concentration of isotopes x or y in a 5.4 M NaCl brine (values reported in Table 5); $P^{x,y}$ is the crustal production rate of the isotope x or y in the reservoir rock (Table 5); ρ_r an ρ_w are the density of rock (2.7 g cm^{-3}) and the brine (1.1 g cm^{-3}); Λ is the release efficiency from the rock matrix into the brine (assumed to be unity); ϕ is the porosity of the rock reservoir (5% for the dolomite; Bertrand et al., 2003); t the residence time of the brine into the reservoir.

Due to high Mg content, production of nucleogenic Ne might be significant in the dolomite reservoir and lead to the observed $^{21}Ne/^{22}Ne$ ratio values in 200 Ma assuming homogenous production over the entire formation (Fig. 8). Occurrence of large nucleogenic $^{21}Ne^*$ amounts measured in the magmatic rocks of the Monteregian Hills (white squares, Fig. 4; Sasada et al., 1997), clearly suggest that production of $^{21}Ne^*$ is feasible within the St-Lawrence Lowlands. However, *in situ* production rates of $^{38}Ar^*$ and $^{36}Ar^*$ in the sedimentary reservoirs (Fig. 8), Grenville basement or the Monteregian Hills (Table 5) all are equally capable of reproducing isotopic ratios close (similar) to the initial atmospheric one (Fig. 8).

By studying the distribution of $^{20}Ne/^{22}Ne$ and $^{21}Ne/^{22}Ne$ in crustal fluids, Kennedy et al. (1990) noted that the expected Ne production ratios in the crust require O/F values far different from average crustal values. Kennedy et al. (1990) concluded that Ne isotopic values in crustal fluids reflect the average O/F ratios of the mineral environment in which the U and Th are sited (mainly mica and amphibole), rather than the average crustal or sedimentary values. High $^{21}Ne/^{22}Ne$ and $^{38}Ar/^{36}Ar$ ratios have been measured in U–Th–Cl–F-rich accessory minerals such as fluorite, apatite or pitchblende (Eikenberg et al., 1993). Ne and Ar isotopic variations observed in the Bécancour brines lie within the field of production in pitchblende, strongly suggesting that accessory minerals are the sites of production of measured nucleogenic Ne and Ar. However, we should expect some fissiogenic ^{86}Kr and ^{136}Xe together with nucleogenic $^{21}Ne^*$, $^{22}Ne^*$ and $^{38}Ar^*$, $^{36}Ar^*$ (Eikenberg et al., 1993). Some ^{136}Xe might occur in the Bécancour brines (Table 5) but uncertainties on the isotopic ratios are too large to confirm such a hypothesis. The anomalies in Ar isotopes need to be further investigated but they point out to specific production of nucleogenic noble gases in U–Th–Cl–F-rich accessory minerals.

Production and sources of radiogenic noble gases in the Bécancour brines might also be evaluated by examining the radiogenic ratios $^4He/^{40}Ar^*$ and $^{21}Ne^*/^{40}Ar^*$. However, the original ratios are expected to fractionate during degassing processes at the wellhead as observed for the atmospheric elemental ratios (Fig. 6). The corrected $^4He/^{40}Ar^*$ and $^{21}Ne^*/^{40}Ar^*$ ratios of the brines prior to fractionation can be approximated to a first order as follows (Pinti and Marty, 1995):

$$\left(\frac{^4He}{^{40}Ar^*}\right)_{corrected} \cong \left(\frac{^{20}He}{^{40}Ar^*}\right)_{measured} \times \frac{(^{20}Ne/^{36}Ar)_{ASB}}{(^{20}Ne/^{36}Ar)_{measured}} \quad (11)$$

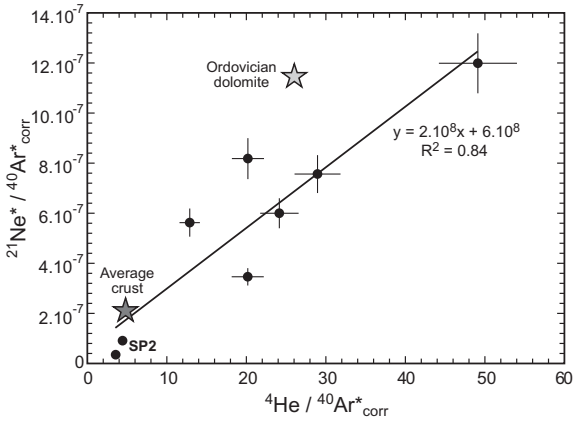

Fig. 9. Correlation between the $^4He/^{40}Ar^*$ and $^{21}Ne^*/^{40}Ar^*$ radiogenic ratios corrected for the mass fractionation produced by brine degassing. The correlation likely describes the mixing between two sources of radiogenic gases, namely the crystalline basement and *in situ* production within a sedimentary reservoir. End-members representing theoretical $^4He/^{40}Ar^*$ and $^{21}Ne^*/^{40}Ar^*$ ratios in the upper crust and in the Ordovician dolomite are from Table 5.

$$\left(\frac{^{21}Ne^*}{^{40}Ar^*}\right)_{corrected} \cong \left(\frac{^{21}Ne^*}{^{40}Ar^*}\right)_{measured} \times \frac{(^{20}Ne/^{36}Ar)_{ASB}}{(^{20}Ne/^{36}Ar)_{measured}} \quad (12)$$

From Fig. 9 it is apparent that both corrected $^4He/^{40}Ar^*$ and $^{21}Ne^*/^{40}Ar^*$ ratios are correlated. This correlation can be interpreted either as the dilution of a radiogenic source by an atmospheric component, i.e., $^4He/^{40}Ar^*$ and $^{21}Ne^*/^{40}Ar^* = 0$, or the mixing between two radiogenic sources. The first hypothesis can be discarded because the sample with the lowest $^4He/^{40}Ar^*$ and $^{21}Ne^*/^{40}Ar^*$ ratios (lower left corner, Fig. 9) are the SP2 brines, which contain the highest amounts of radiogenic noble gases (Table 2). Thus, mixing between two radiogenic sources is likely responsible for the observed $^4He/^{40}Ar^* - ^{21}Ne^*/^{40}Ar^*$ correlation. The first source show $^4He/^{40}Ar^*$ and $^{21}Ne^*/^{40}Ar^*$ ratios (lower left of Fig. 9) close to that of an average upper crust or those calculated for the gneiss-amphibolite complexes of the Grenville basement or Monteregian Hills gabbros and diorites (Table 5). The second source shows $^4He/^{40}Ar^*$ of 50 and $^{21}Ne^*/^{40}Ar^* = 1.2 \times 10^{-6}$ (upper right side, Fig. 9) and could be related to *in situ* production within the St-Lawrence Lowlands sedimentary sequence, i.e., the Ordovician dolomite (Table 5), and possibly fractionated towards higher values by partial retention of $^{40}Ar^*$ in minerals at the reservoir temperature (Ballentine et al., 1994).

5.4. Migration pathways and residence times of the Bécancour brines

Dissolved ions, Sr isotopic composition and noble gases can provide useful constraints on the history of the Bécancour brines, their origin, migration paths and residence times.

The chemistry and noble gas contents of brines suggest the occurrence of extended water-rock interactions that allowed brines to acquire additional Ca and radiogenic Sr (Figs. 2b and 3) in addition to nucleogenic/radiogenic He, Ne and Ar (Figs. 7–9). The most intriguing feature of these brines is the very low bromide content, which cannot be accounted for by seawater evaporation (Fig. 2a). The Cl/Br ratios indicate halite dissolution, i.e., leaching of salt domes. However, evaporite sequences in the Cambrian–Ordovician sedimentary formations of the St-Lawrence Lowlands in Québec or in the Precambrian Shield are not known. Evaporites in Eastern Canada are mainly of Devonian and Silurian age (Ford, 1997). It is possible that the same sequences were present in the St-Lawrence Lowlands in Québec and subsequently eroded. Monteregian Hills were intruded 1.8–2.0 km at depth and presently outcrop on the St-Lawrence plain indicating that a *n* equivalent km-thick sequence of sediments covered the St-Lawrence Lowlands during Cretaceous time (Feininger and Goodacre, 2003). Studies on the thermal maturation of the gas-prone Upper Ordovician Utica Shale indicate that this source rock reached temperatures equivalent to the condensate gas (135–165 °C) to dry gas maturation zones (165–230 °C) during Devonian (Lavoie et al., 2009). Vitrinite reflectance studies of the Utica shales recorded

burial depths varying between 5.6 and 7.5 km (Heroux and Bertrand, 1991). This is agreement also with AFT thermal resetting observed in Precambrain basement rocks sampled along the faults bordering the St-Lawrence Rift System (Roden-Tice and Tremblay, 2009). The thermal resetting suggest that the Grenville rocks now at the surface were formerly buried by a Paleozoic sedimentary sequence to depths more than 5 km. Thus, Bécancour brines could have been formed by water leaching Devonian-Silurian evaporite bodies, which subsequently infiltrated the basin, possibly down to the Grenville basement where acquired the radiogenic Sr (Fig. 3) and the nucleogenic/radiogenic He–Ne–Ar signatures (Figs. 8 and 9).

Another feature of the Bécancour brines capable of placing constraints on their residence time are the radiogenic ^{4}He and $^{40}Ar^{*}$ budgets. The brines display high $^{40}Ar/^{36}Ar$ ratios, up to 2100 (Table 2) and relatively low $^{4}He/^{40}Ar^{*}$ values, from 4 to 50, close to the production ratios in rocks of the Grenville basement or the Ordovician dolostone (Fig. 9). This indicates that both He and Ar have been efficiently released from the rock to the fluids. Release of He and Ar is intimately related to the thermal regime of the basin (Ballentine et al., 1994). Only at temperatures of 250–300 °C should radiogenic ^{4}He and $^{40}Ar^{*}$ be available in the pore fluids at their production ratio. These temperatures approximately correspond to the closure temperature of Ar in mica and K-feldspar (Lippolt and Weigel, 1988). The present-day geothermal gradient in St-Lawrence Lowlands is 15 °C/km (Lamontagne and Ranalli, 1996), indicating that Bécancour brines are well below the Ar closure temperature. Fission-track thermochronology of the St-Lawrence Rift System suggests that the present-day thermal regime could have lasted since Late Jurassic (Roden-Tice and Tremblay, 2009). The St-Lawrence Lowlands could have reached temperatures greater than 250 °C solely during (1) Devonian, when Utica shale matured, producing natural gas (Lavoie et al., 2009); or (2) briefly and locally during Cretaceous Monteregian Hills magmatic episode (Heroux and Bertrand, 1991). This suggests that $^{40}Ar^{*}$ was introduced in the Bécancour brines sometime between these two thermal events.

Devonian ages for the Bécancour brines are not unrealistic. Indeed, Bottomley et al. (2005) elaborated a similar hypothesis to justify the origin of the Canadian Precambrian Shield brines. These brines might have been derived from seawater evaporation and infiltration of the residual brine during the Devonian, when seawater inundated extensive areas of the presently exposed shield region. Recent U–Th–^{4}He ages of Precambrian shield brines at Yellowknife seem to confirm a Devonian age there also (Greene et al., 2008). Younger Cretaceous ages for brines are consistent with the occurrence of mantle-derived ^{3}He in Bécancour brines (Fig. 7), possibly leached from local alkaline intrusions related to the Monteregian Hills (Faure et al., 1996). Such an environment would be better suited to find accessory minerals such as apatite where nucleogenic $^{38}Ar^{*}$, $^{36}Ar^{*}$ and $^{21}Ne^{*}$, $^{22}Ne^{*}$ could be produced over time (Fig. 8). If Bécancour brines are younger than the Cretaceous, Precambrian basement would have then contributed exclusively to their nucleogenic/radiogenic noble gas budget (Torgersen, 1993; Ma et al., 2009). However, leaching of halogens from accessory minerals such as apatite (Frape et al., 2003) cannot constitute a viable source for the large salinities observed in the Bécancour brines.

6. CONCLUSIONS

The source of salinity of Na–Ca–Cl brines residing in the Cambrian–Ordovician sedimentary sequence of the St-Lawrence Lowlands, Québec seems to be related to halite dissolution. The brines contain a mixture of radiogenic/nucleogenic He, Ne, and Ar together with a small amount of mantle-derived ^{3}He component. Nucleogenic $^{21}Ne^{*}$ and $^{22}Ne^{*}$ are possibly accompanied by nucleogenic $^{38}Ar^{*}$ produced in Cl–F-rich accessory minerals, together with a large amount of radiogenic ^{4}He and $^{40}Ar^{*}$ derived from the decay of U, Th, and K. The crystalline basement is the most suitable source of brine radiogenic/nucleogenic noble gas budget and very long water–rock interactions with such an environment could also explain the measured highly radiogenic Sr isotopic signature (Fig. 3) and the Ca excesses (Fig. 2b). The $^{4}He/^{40}Ar^{*}$ and $^{21}Ne/^{40}Ar^{*}$ ratios, corrected for brine degassing fractionation are close to their production ratios in rocks, suggesting that ^{4}He and $^{40}Ar^{*}$ were released efficiently from rock to fluids at reservoir temperature higher than 250 °C. These temperatures could have been reached only during the Devonian, when Utica shale matured producing large amounts of natural gas or locally, during the Cretaceous Monteregian Hills magmatic pulse, contributing mantle-^{3}He to brines. A Devonian age for these brines is compatible with the age of evaporite deposits in the region that could be the source of their salinity.

ACKNOWLEDGEMENTS

Thoughtful reviews of M.C. Van Soest, M. Kendrick, an anonymous reviewer and the associate editor Bernard Marty largely improved the manuscript. Discussions on the salinity origin of brines with Orfan Shouakar-Stash (Waterloo Un.) were appreciated. We wish to thank G. Bach, F. Pitre and Luc Massé for helping during sampling. We wish to thanks all JUNEX's people for helping and supporting us at the Bécancour site. M. Laithier improved our illustrations. Research funding to CBO were provided by a NSERC Industrial fellowship (Contract No. 342297) and JUNEX Inc. Financial support to D.L.P. was from NSERC Discovery Grant (Nos. 376110 and 314496); to A.T. from NSERC Discovery Grant (No. PG-105669). This is GEOTOP Contribution No. 2011-003.

REFERENCES

Andrews J. N. and Kay R. L. F. (1982) Natural production of tritium in permeable rocks. *Nature* **298**, 361–363.

Andrews J. N., Davis S. N., Fabryka-Martin J., Fontes J.-Ch., Lehmann B. E., Loosli H. H., Michelot J.-L., Moser H., Smith B. and Wolf M. (1989) The in situ production of radioisotopes in rock matrices with particular reference to the Stripa granite. *Geochim. Cosmochim. Acta* **53**, 1803–1815.

Ballentine C. J., Mazurek M. and Gautschi A. (1994) Thermal constraints on crustal rare gas release and migration: evidence from Alpine fluid inclusions. *Geochim. Cosmochim. Acta* **58**, 4333–4348.

Ballentine C. J. and Burnard P. G. (2002) Production, release and transport of noble gases in the continental crust. *Rev. Mineral. Geochem.* **47**, 481–538.

Bertrand R., Chagnon A., Malo M., Duchaine Y., Lavoie D. and Savard M. M. (2003) Sedimentologic, diagenetic and tectonic evolution of the Saint-Flavien gas reservoir at the structural front of the Quebec Appalachians. *Bull. Can. Petrol. Geol.* **51**, 126–154.

Bosch A. and Mazor E. (1988) Natural gas association with water and oil as depicted by atmospheric noble gases: case studies from the southeastern Mediterranean Coastal Plain. *Earth Planet Sci. Lett.* **87**, 338–346.

Bottomley D., Clark I., Battye N. and Kotzer T. (2005) Geochemical and isotopic evidence for a genetic link between Canadian Shield brines, dolomitization in the western Canada sedimentary basin, and Devonian calcium-chloride seas. *Can. J. Earth Sci.* **42**, 2059–2071.

Carpenter A. B. (1978) Origin and chemical evolution of brines in sedimentary basins. *Oklahoma Geol. Surv. Circ.* **79**, 60–77.

Castro M. C., Jambon A., de Marsily G. and Schlosser P. (1998a) Noble gases as natural tracers of water circulation in the Paris Basin 1. Measurements and discussion of their origin and mechanisms of vertical transport in the basin. *Water Resour. Res.* **34**, 2443–2466.

Castro M. C., Goblet P., Ledoux E., Violette S. and de Marsily G. (1998b) Noble gases as natural tracers of water circulation in the Paris Basin 2. Calibration of a groundwater flow model using noble gas isotope data. *Water Resour. Res.* **34**, 2467–2483.

Castro M. C., Ma L. and Hall C. M. (2009) A primordial, solar He–Ne signature in crustal fluids of a stable continental region. *Earth Planet. Sci. Lett.* **279**, 174–184.

Cawood P. A., McCausland P. J. A. and Dunning G. R. (2001) Opening Iapetus: constraints from the Laurentian margin in Newfoundland. *Geol. Soc. Am. Bull.* **113**, 443–453.

Chao G. Y. and Ercit S. T. (1991) Nalipoite, sodium dilithium phosphate, a new mineral species from Mont Saint-Hilaire. *Québec. Can. Miner.* **29**, 565–568.

Davisson M. L. and Criss R. E. (1996) Na–Ca–Cl relations in basinal fluids. *Geochim. Cosmochim. Acta* **60**, 2743–2752.

Eby G. N. (1985) Age relations, chemistry, and petrogenesis of mafic alkaline dikes from the Monteregian Hills and younger White Mountain igneous provinces. *Can. J. Earth Sci.* **22**, 1103–1111.

Eikenberg J., Signer P. and Wieler R. (1993) U–Xe, U–Kr, and U–Pb systematics for dating uranium minerals and investigations of the production of nucleogenic neon and argon. *Geochim. Cosmochim. Acta* **57**, 1053–1069.

Fanale F. P. and Cannon W. A. (1972) Origin of planetary primordial rare gas: the possible role of adsorption. *Geochim. Cosmochim. Acta* **36**, 319–328.

Faure S., Tremblay A. and Angelier J. (1996) State of intraplate stress and tectonism of northeastern America since Cretaceous times, with particular emphasis on the New England–Quebec igneous province. *Tectonophysics* **255**, 111–134.

Feininger T. and Goodacre A. (2003) The distribution of igneous rocks beneath Mont Mégantic (the easternmost Monteregian) as revealed by gravity. *Can. J. Earth Sci.* **40**, 765–773.

Fontes J-Ch., Andrews J. N. and Walgenwitz F. (1991) Évaluation de la production naturelle *in situ* d'argon-36 via le chlore-36: implications géochimiques et géochronologiques. *C. R. Acad. Paris* 313, Série II, 649–654.

Fontes J.-Ch. and Matray J.-M. (1993) Geochemistry and origin of formation brines from the Paris Basin. Part 2 Saline solutions associated with oil fields. *Chem. Geol.* **109**, 177–200.

Ford D. C. (1997) Principal features of evaporite karst in Canada. *Carbonates Evaporites* **12**, 15–23.

Franklyn M., McNutt R., Kamineni D., Gascoyne M. and Frape S. (1991) Groundwater $^{87}Sr/^{86}Sr$ values in the Eye-Dashwa Lakes pluton, Canada: Evidence for plagioclase-water reaction. *Chem. Geol.* **86**, 111–122.

Frape S. K., Blyth A., Blomqvist R., McNutt R. H., Gascoyne M., Heinrich D. H. and Karl K. T. (2003) *Deep Fluids in the Continents: II. Crystalline Rocks*. Treatise on Geochemistry, Pergamon, Oxford.

Greene S., Battye N., Clark I. D., Kotzer T. and Bottomley D. (2008) Canadian Shield brine from the Con Mine, Yellowknife, NT, Canada: Noble gas evidence for an evaporated Palaeozoic seawater origin mixed with glacial meltwater and Holocene recharge. *Geochim. Cosmochim. Acta* **72**, 4008–4019.

Hanor J. S. (1994) Origin of saline fluids in sedimentary basins. In *Geofluids: Origin, Migration, and Evolution of Fluids in Sedimentary Basins* (ed. J. Parnell), Geol. Soc. Spec. Pub. 78, pp.151–174.

Heroux Y. and Bertrand R. (1991) Maturation thermique de la matière organique dans un bassin du Paléozoïque inférieur, basses-terres du Saint-Laurent, Québec, Canada. *Can. J. Earth Sci.* 28, 1019–1030.

Hobbs M. Y., Frape, S. K., Shouakar-Stash O. and Kennell L. R. (2011) *Regional Hydrogeochemistry – Southern Ontario*. Nuclear Waste Management Organization, Report no. NWMO DGR-TR-2011-12, pp. 156.

Jähne B., Heinz G. and Dietrich W. (1987) Measurement of the diffusion coefficients of sparingly soluble gases in water. *J. Geophys. Res.* **92**, 10,767–10,776.

Kennedy B. M., Hiyagon H. and Reynolds J. H. (1990) Crustal neon: a striking uniformity. *Earth Planet. Sci. Lett.* **98**, 277–286.

Kharaka Y. K., Hanor J. S., Heinrich D. H. and Karl K. T. (2003) *Deep Fluids in the Continents: I. Sedimentary Basins*. Treatise on Geochemistry, Pergamon, Oxford.

Lamontagne M. and Ranalli G. (1996) Thermal and rheological constraints on the earthquake depth distribution in the Charlevoix, Canada, intraplate seismic zone. *Tectonophysics* **257**, 55–69.

Lavoie D., Pinet N., Dietrich J., Hannigan P., Castonguay S., Hamblin A. P. and Giles P. (2009) *Petroleum Resource Assessment, Paleozoic successions of the St. Lawrence Platform and Appalachians of eastern Canada*. Geological Survey of Canada, Open File 6174, pp. 275.

Lippolt H. J. and Weigel E. (1988) ^{4}He diffusion in ^{40}Ar-retentive minerals. *Geochim. Cosmochim. Acta* **56**, 1569–1590.

Ma L., Castro M. C., Hall C. M. and Walter L. M. (2005) Cross-formational flow and salinity sources inferred from a combined study of helium concentrations, isotopic ratios, and major elements in the Marshall aquifer, southern Michigan. *Geochem. Geophys. Geosyst.* **6**. doi:10.1029/2005GC001010.

Ma L., Castro M. C. and Hall C. M. (2009) Crustal noble gases in deep brines as natural tracers of vertical transport processes in the Michigan Basin. *Geochem. Geophys. Geosyst.* **10**. doi:10.1029/2009GC002475.

Mamyrin B. A. and Tolstikhin I. N. (1984) *Helium Isotopes in Nature*. Elsevier, Amsterdam.

Marty B. (1984) On the noble gas isotopic fractionation in naturally occurring gases. *Geochem. J.* **18**, 157–162.

Marty B., Torgersen T., Meynier V., O'Nions R. K. and de Marsily G. (1993) Helium isotope fluxes and groundwater ages in the Dogger aquifer, Paris Basin. *Water Resour. Res.* **29**, 1025–1036.

Matsuda J. and Nagao K. (1986) Noble gas abundances in a deep-sea sediment core from eastern equatorial Pacific. *Geochem. J.* **20**, 71–80.

Matsuda J. and Matsubara K. (1989) Noble gases in silica and their implications for the terrestrial "missing" Xe. *Geophys. Res. Lett.* **16**, 81–84.

Matsumoto T., Honda M., McDougall I., Yatsevich I. and O'Reilly S. Y. (2004) Isotope fractionation of neon during stepheating extraction? A comment on 'Re-interpretation of the existence of a primitive plume under Australia based on neon isotope fractionation during step heating' by Gautheron and Moreira (2003). *Terra Nova* **16**, 23–26.

McHone J. G. (1996) Constraints on the mantle plume model for mesozoic alkaline intrusions in northeastern North America. *Can. Mineral.* **34**, 325–334.

McNutt R., Frape S. and Dollar P. (1987) A strontium, oxygen and hydrogen isotopic composition of brines, Michigan and Appalachian Basins, Ontario and Michigan. *Appl. Geochem.* **2**, 495–505.

Ministère québécois des Ressources naturelles, de la Faune et des Parcs (2005). Site SIGEOM at <http://www.mrnfp.gouv.qc.ca/produits-services/mines.jsp>.

Négrel P. and Casanova J. (2005) Comparison of the Sr isotopic signatures in brines of the Canadian and Fennoscandian shields. *Appl. Geochem.* **20**, 749–766.

Owen V. J. and Greenough J. D. (2008) Influence of Potsdam sandstone on the trace element signatures of some 19th-century American and Canadian glass: Redwood, Redford, Mallorytown, and Como–Hudson. *Geoarchaeology* **23**, 587–607.

Ozima M. and Podosek F. A. (1983) *Noble Gas Geochemistry*. Cambridge University Press, Cambridge.

Pinti D. L. and Marty B. (1995) Noble gases in crude oils from the Paris Basin, France: implications for the origin of fluids and constraints on oil–water–gas interactions. *Geochim. Cosmochim. Acta* **59**, 3389–3404.

Pitre F. and Pinti D. L. (2010) Noble gas enrichments in porewater of estuarine sediments and their effect on the estimation of net denitrification rates. *Geochim. Cosmochim. Acta* **74**, 531–539.

Rivard P., Ollivier J.-P. and Ballivy G. (2002) Characterization of the ASR rim: application to the Potsdam sandstone. *Cem. Concr. Res.* **32**, 1259–1267.

Roden-Tice M. and Tremblay A. (2009) Post-Jurassic uplift and faulting along the St. Lawrence rift system, Québec based on apatite fission-track evidence. *Geol. Soc. America Abstracts with Programs* **41**, 33.

Sano Y., Nagao K. and Pillinger C. T. (1994) Carbon and noble gases in Archean chert. *Chem. Geol.* **112**, 327–342.

Sarda P., Staudacher T. and Allègre C. J. (1988) Neon isotopes in submarine basalts. *Earth Planet. Sci. Lett.* **91**, 73–88.

Sasada T., Hiyagon H., Bell K. and Ebihara M. (1997) Mantle-derived noble gases in carbonatites. *Geochim. Cosmochim. Acta* **61**, 4219–4228.

Siegel D. I., Lesniak K. A., Stute M. and Frape S. (2004) Isotopic geochemistry of the Saratoga springs: implications for the origin of solutes and source of carbon dioxide. *Geology* **32**, 257–260.

Sleep N. (1990) Monteregian hotspot track: a long-lived mantle plume. *J. Geophys. Res.* **95**, 21983–21990.

Smith S. P. and Kennedy B. M. (1983) The solubility of noble gases in water and NaCl brine. *Geochim. Cosmochim. Acta* **47**, 503–515.

Tolstikhin I. N., Lehmann B. E., Loosli H. H. and Gautschi A. (1996) Helium and argon isotopes in rocks, minerals, and related groundwaters: a case study in northern Switzerland. *Geochim. Cosmochim. Acta* **60**, 1497–1514.

Torgersen T. (1993) Defining the role of magmatism in extensional tectonics – helium-3 fluxes in extensional basins. *J. Geophys. Res.* **98**, 16257–16269.

Torgersen T., Drenkard S., Stute M. and Schlosser P. (1995) Mantle helium in ground waters of eastern North America; time and space constraints on sources. *Geology* **23**, 675–678.

Torgersen T. and Kennedy B. M. (1999) Air–Xe enrichments in Elk Hills oil field gases: role of water in migration and storage. *Earth Planet. Sci. Lett.* **167**, 239–253.

Tremblay A. and Castonguay S. B. (2002) Structural evolution of the Laurentian margin revisited (southern Quebec Appalachians): implications for the Salinian orogeny and successor basins. *Geology* **30**, 79–82.

Tremblay A., Long B. and Masse M. (2003) Supracrustal faults of the St. Lawrence rift system, Quebec: kinematics and geometry as revealed by field mapping and marine seismic reflection data. *Tectonophysics* **369**, 231–252.

Veizer J. N. et al. (1999) $^{87}Sr/^{86}Sr$, $\delta^{13}C$ and $\delta^{18}O$ evolution of Phanerozoic seawater. *Chem. Geol.* **161**, 59–88.

Weiss R. F. (1968) Piggybacks sampler for dissolved gas studies on sealed water tubes. *Deep Sea Res.* **15**, 695–699.

Wetherill G. W. (1954) Variations in the isotopic abundances of neon and argon extracted from radioactive minerals. *Phys. Rev.* **96**, 679–683.

Associate editor: Bernard Marty